Gateway states and bath states in the vibrational spectrum of H_3^+

C. Ruth Le Sueur, James R. Henderson [1] and Jonathan Tennyson
Department of Physics & Astronomy, University College London, Gower Street, London WC1E 6BT, UK

Received 7 November 1992; in final form 1 March 1993

Vibrational band intensities are obtained from discrete variable representation calculations of eigenstates for H_3^+. Transitions linking highly excited states to the ground state show large variations in intensities, with gateway states corresponding to highly excited bending motion ("horseshoes") which leak intensity into the nearby bath states. It is suggested that these gateway states may be observable. Implications of these results for the interpretation of the infrared predissociation spectra of H_3^+ are discussed.

1. Introduction

There is a great deal of interest in H_3^+: after an initial dearth of assigned transitions, experiments and observations have lately come thick and fast. To a large extent, the paucity of assigned lines arose from the fact that there were no good indications as to where to look for the lines. Recently, however, the availability of an extremely high-accuracy ab initio electronic potential energy surface due to Meyer, Botschwina and Burton (MBB) [1], has enabled the position of transitions to be pinpointed with great accuracy. The latest and most accurate calculation using this surface, for example, boasts that all the bound vibrational band levels are converged to within 2 cm^{-1} [2]. Furthermore, this surface was also used for ab initio calculations of rovibrational levels which enabled the assignment of a spectrum emanating from Jupiter [3].

Carrington and Kennedy observed a very complex spectrum of H_3^+, with over 27000 lines in 220 cm^{-1}. This spectrum, which results from transitions between highly excited metastable rovibrational states, has so far eluded explanation, implying perhaps that the molecule at these energies may be completely chaotic in its motions. However, by convoluting the stronger lines to obtain a pseudo coarse-grained spectrum, they observed four broad bands, at 1033.62, 978.45, 928.02 and 875.65 cm^{-1}, indicating that there is at least some regular behaviour underlying this spectrum.

Over the years since that spectrum was first observed, there have been many attempts to explain these four bands. At first Carrington and co-workers noted the fact that they correlated well with $N=5\leftarrow3$ rotational transitions in H_2 with 0, 1, 2 and 3 quanta of stretch, but nothing more came of this suggestion [4,5]. The currently favoured explanation is that the four broad bands are due to rotational transitions in the R branch of highly excited vibrational states. It has been noted that all the vibrational levels of H_3^+ have roughly the same rotational constants of approximately 25 cm^{-1}, which would imply a spacing between consecutive rotational transitions of roughly 50 cm^{-1} [6]. This is in reasonable agreement with the observed spacings. The only question remaining is what states are long lived enough to be observed. The most likely candidate states are the "horseshoe" states [7] in which the complex undergoes what are in effect large amplitude bending motions of a quasi-linear molecule.

Although there have been many calculations of H_3^+ energy levels (see, for example, refs. [8–13] for calculations extending above the barrier to linearity), calculations of transition intensities are very much rarer. The assignment of the Jupiter spectrum was one case where transition intensities were invaluable, enabling a spectrum to be generated in extremely good agreement with the observed data [3].

[1] Current address: ULCC, 20 Guilford Street, London WC1N 1DZ, UK.

Calculating transition intensities between energy levels for a highly excited molecule, however, would produce too much data to be useful, and in any case at this stage the data would probably not be reliable enough to place much credence on it. One option is to calculate intensities for vibrational bands, rather than for the individual rovibrational transitions within these bands. The correct method of doing this has recently been outlined by Le Sueur et al. [14]. The theory relies on an approximation which is only valid when the molecule is in a configuration close to equilibrium, but the transition intensities it generates are in good agreement with other calculations (see below). In this work we present results obtained using DVR (discrete variable representation) calculations of H_3^+ eigenstates. In particular we focus on transition moments linking low-lying vibrational states to high-lying levels in the ion. These transitions lie in the near infrared and optical range and we suggest many may be observable. The only comparably previous studies have been restricted to vibrational states below linearity [15,16].

2. Theory

2.1. Evaluation of the transition moment

When a DVR calculation of eigenvalues is performed, the resultant wavefunctions are not expressed as a linear combination of functions, but as a set of amplitudes at points in configuration space. Evaluating the expectation value of an operator which commutes with the wavefunction is therefore very simple within the quadrature approximation [17],

$$\langle\psi|\hat{O}|\psi\rangle=\sum_{\alpha,\beta,\gamma}\psi_{\alpha,\beta,\gamma}\hat{O}_{\alpha,\beta,\gamma}\psi_{\alpha,\beta,\gamma}\,, \tag{1}$$

where (α, β, γ) specifies a position in three-dimensional configuration space (these expressions are easily generalisable to n dimensions). The vibrational band transition moment, however, which is defined [14,18] as

$$S_{\mathrm{fi}}^{\mathrm{vib}}=|\langle\psi_{\mathrm{f}}|\boldsymbol{\mu}^{\mathrm{E}}|\psi_{\mathrm{i}}\rangle|^2\,, \tag{2}$$

is not necessarily so easy to evaluate. The complication arises from the fact that the amplitudes ψ_{f} and ψ_{i} may not have been calculated at the same points. In such cases it is necessary to decide how to evaluate the expression, given that the quadrature approximation can no longer be used directly. The wavefunctions must now be re-expressed in terms of functions using the transformation tensor, T, giving the complete integral as

$$\begin{aligned}\langle\psi_{\mathrm{f}}|\boldsymbol{\mu}^{\mathrm{E}}|\psi_{\mathrm{i}}\rangle=&\sum_{\substack{\alpha\beta\gamma\\ \alpha'\beta'\gamma'}}\psi_{\mathrm{f}\alpha,\beta,\gamma}\psi_{\mathrm{i}\alpha',\beta',\gamma'}\\ &\times T^{l,m,n}_{\alpha,\beta,\gamma}T^{l',m',n'}_{\alpha',\beta',\gamma'}\int\boldsymbol{\mu}^{\mathrm{E}}_{x,y,z}f_l(x)f'_{l'}(x)\\ &\times g_m(y)g'_{m'}(y)h_n(z)h'_{n'}(z)\,\mathrm{d}x\,\mathrm{d}y\,\mathrm{d}z\,,\end{aligned} \tag{3}$$

where f, g, h, f', g' and h' are the basis functions used for the bra and ket respectively (typically, these will be Legendre and Laguerre polynomials), and $T^{l,m,n}_{\alpha,\beta,\gamma}=\omega_\alpha^{1/2}f_l(x_\alpha)\omega_\beta^{1/2}g_m(y_\beta)\omega_\gamma^{1/2}h_n(z_\gamma)$. ω_α is the weight associated with the αth quadrature point x_α. A decision must be taken as to how the integral on the right-hand side of this equation can be evaluated. If the functions f, g and h have the same metrics as the functions f', g' and h', then the simplest procedure is to use the same quadrature schemes as resulted in the original DVR points for the two wavefunctions, and to take the average of the results so obtained. If this is not the case, a quadrature scheme must be chosen so that integrals of both types of functions can be evaluated properly. A sensible way to choose this quadrature scheme is to ensure that overlap integrals over products of the functions are evaluated properly, i.e. that within the quadrature scheme, functions are still orthonormal. This is effectively the same as ensuring that the quadrature approximation is still valid for the special case where the bra and ket functions are not the same.

A set of polynomials $f_n(x)$ which are orthogonal over a metric $w(x)$,

$$\int w(x)f_n(x)f_m(x)\,\mathrm{d}x=0,\quad n\neq m\,, \tag{4}$$

can be numerically exactly integrated using a quadrature scheme based on the zeros of $f_N(x)$ $(N>n, m)$,

$$\int w(x)f_n(x)f_m(x)\,\mathrm{d}x=\sum_{\alpha=1}^{N}\omega_\alpha f_n(x_\alpha)f_m(x_\alpha)\,. \tag{5}$$

In order to numerically exactly integrate them using a different quadrature scheme, based on, say, a set

of polynomials $g_n(x)$ which are orthogonal over a different metric $W(x)$,

$$\int w(x) f_n(x) f_m(x)\,\mathrm{d}x = \int W(x)\left(\frac{w(x)}{W(x)} f_n(x) f_m(x)\right)\mathrm{d}x = \sum_{\alpha=1}^{M} \Omega_\alpha \frac{w(x_\alpha)}{W(x_\alpha)} f_n(x_\alpha) f_m(x_\alpha)\,, \quad (6)$$

the products $[w(x)/W(x)]f_n(x)f_m(x)$ must all be expressible as linear combinations of a finite number of products $g_n(x)g_m(x)$ (and hence as polynomials of order $n+m$). If that is true then the x_α must be the zeros of the polynomial $g_M(x)$ whose order M is greater than that of any polynomial $g_n(x)$ involved in the linear combinations.

2.2. Eckart axes

It has been shown previously [14] that in order to calculate vibrational band intensities from variational wavefunctions, it is necessary to refer the dipole surface to the Eckart coordinate system [19]. This coordinate system is defined as one in which the position vectors of the atoms obey the following relationships:

$$\sum_{i=1}^{n} m_i \boldsymbol{r}_i = \boldsymbol{0}, \quad \sum_{i=1}^{n} m_i \boldsymbol{r}_i \times \boldsymbol{r}_i^{\mathrm{e}} = \boldsymbol{0}\,, \quad (7)$$

where $\boldsymbol{r}_i^{\mathrm{e}}$ denotes the position vector of atom i at equilibrium. The first of these merely places the origin of the coordinate system at the centre of mass. The latter ensures that the angular momentum in this coordinate system is approximately constant. Clearly these relationships will hold in any of an infinite set of coordinate systems related by a fixed rotation about the centre of mass, and so referring dipoles to the Eckart coordinate system is simple. One simply places the Eckart axes parallel to the original internal axes at equilibrium, and then calculates how much the Eckart axes rotate with respect to the original axes at each position away from equilibrium [14]. This technique is particularly suited to DVR calculations where all integrations are done using quadrature.

It must be noted that the Eckart conditions were derived by assuming that the molecule undergoes only small deviations from equilibrium, and so this technique may not be appropriate for looking at the intensities of transitions between large amplitude modes. Nevertheless, tests performed earlier [14] show that, certainly for transitions involving low-lying states, the calculations are reasonably accurate. One good test is to observe when the symmetry-based selection rules break down. The results presented in this paper show that the A coefficients for forbidden (A↔A) transitions are typically several orders of magnitude lower than those for allowed transitions, at least in the range where symmetry assignments are firm.

3. Calculations

The eigenstates of H_3^+ used in this Letter were produced earlier [2], using the DVR3D program [20] and implementation A [21] of the MBB potential [1]. The calculation was done in scattering coordinates, with internal coordinates r_1, the H–H distance, r_2, the scattering length (the distance from the midpoint of r_1 to the third atom), and θ the angle between r_1 and r_2. The full symmetry of H_3^+ was not used, but the Hamiltonian was split into two blocks according to whether even or odd combinations of $\psi(\theta)$ and $\psi(\pi-\theta)$ were taken. The coordinates were treated in the order $\theta \rightarrow r_1 \rightarrow r_2$, with 32, 36 and 40 points respectively. The Hamiltonian was truncated between treatment of each coordinate using an energy criterion (so that intermediate solutions with very high energies were ignored), with a final matrix size of 6500. The resulting eigenstates are orthogonal to within the precision of the machine (i.e. to 13 decimal places)

Since it is possible for this system to become linear at relatively low energies (about 12000 cm^{-1} above the vibrational ground state), it was necessary to use functions for the scattering length, r_2, which behaved correctly at r_2, which behaved correctly at $r_2=0$. Spherical oscillator functions of the type

$$2^{1/2}\beta^{1/4} N_{n\alpha+1/2} \exp(-\tfrac{1}{2}x) x^{(\alpha+1)/2} L_n^{\alpha+1/2}(x)\,, \quad x=\beta r_2^2\,, \quad (8)$$

were therefore used, where $L_n^{\alpha+1/2}(x)$ is an associated Laguerre polynomial. Henderson et al. [2]

Table 1
A comparison of A coefficients in s^{-1}. The top row indicates who did the work and the second row gives the dipole surface used. Vibrational states are assigned as (v_1, v_2^l)

Transition	Frequency (cm^{-1})	CP [15] CP [15]	DMT [16] MBB [1]	This work		
				MBB	MBB (corrected)	ref. [22]
$(0,0^0)\leftarrow(0,1^1)$	2521.3	124.0	128.8	128.9/128.9	128.8/128.8	120.5/120.5
$(0,0^0)\leftarrow(0,2^2)$	4997.4	174.0	144.6	149.4/154.7	149.3/149.3	167.5/167.5
$(0,0^0)\leftarrow(1,1^1)$	5553.7	1.5	0.3	0.4/0.5	0.4/0.4	16.6/16.6
$(0,0^0)\leftarrow(1,0^0)$	3178.3	forbidden		1.2×10^{-5}	1.8×10^{-11}	5.2×10^{-12}
$(0,0^0)\leftarrow(0,2^0)$	4777.0	forbidden		1.2×10^{-3}	2.6×10^{-9}	3.8×10^{-9}
$(0,0^0)\leftarrow(2,0^0)$	6262.0	forbidden		7.6×10^{-5}	1.2×10^{-13}	6.8×10^{-13}
$(0,1^1)\leftarrow(0,2^2)$	2476.1	253.0	256.0	255.7/256.8	255.4/255.4	218.6/218.6

Table 2
Assignments of the upper levels of the bright transitions observed in fig. 1

No. of quanta in horseshoe mode	State No. (even/odd)	Frequency (cm^{-1}) (even/odd)	A coefficient to ground state (even/odd) (s^{-1})	
			MBB	ref. [22]
1	2/1	2521/2521	128.8/128.8	120.5/120.5
2	5/2	4997/4997	149.3/149.3	167.5/167.5
3	8/4	7003/7003	16.5/16.5	37.9/37.9
4	14/8	9108/9108	6.55/6.55	12.6/12.6
5	21/13	10853/10853	2.17/2.17	5.2/5.2
6	28/18	12294/12294	0.67/0.67	1.4/1.4
7	38/25	13681/13681	0.56/0.56	1.6/1.6
8	50/33	15103/15103	0.29/0.29	0.96/0.96
9	66/47	16712/16712	0.13/0.13	0.23/0.23
10	86/64	18432/18431	$6.0\times10^{-2}/6.0\times10^{-2}$	0.14/0.14
11	115/87	20238/20238	$2.5\times10^{-2}/2.5\times10^{-2}$	$6.4\times10^{-2}/6.3\times10^{-2}$
12	148/115	22115/22115	$1.1\times10^{-2}/1.1\times10^{-2}$	$2.0\times10^{-2}/2.0\times10^{-2}$
13	193/155	24034/24033	$7.7\times10^{-3}/7.7\times10^{-3}$	$1.4\times10^{-2}/1.4\times10^{-2}$
14	244/198	25912/25912	$3.3\times10^{-3}/3.3\times10^{-3}$	$5.6\times10^{-3}/5.7\times10^{-3}$
15	308/256	27803/27803	$1.8\times10^{-3}/1.8\times10^{-3}$	$3.7\times10^{-3}/3.7\times10^{-3}$
16	383/324	29707/29707	$8.1\times10^{-4}/8.5\times10^{-4}$	$1.3\times10^{-3}/1.4\times10^{-3}$
17	470/403	31551/31548	$8.6\times10^{-4}/8.3\times10^{-4}$	$1.3\times10^{-3}/1.2\times10^{-3}$
18	567/491	33301/33297	$3.5\times10^{-4}/5.3\times10^{-4}$	$4.7\times10^{-4}/7.3\times10^{-4}$
19	682/597	35036/35026	$2.3\times10^{-4}/3.5\times10^{-4}$	$3.0\times10^{-4}/4.7\times10^{-4}$
20	819/722	36757/36737	$8.5\times10^{-5}/9.7\times10^{-5}$	$1.1\times10^{-4}/1.3\times10^{-4}$

found that in order to obtain the best convergence, α needs to be 0 and 1 for the even and odd blocks respectively. The metrics for these two sets of functions are $e^{-x}x^{1/2}$ and $e^{-x}x^{3/2}$, neither of which can be represented as a linear function of the other, and so a mutually satisfactory quadrature scheme must be found using the theory outlined above. The simplest method is to search for a quadrature scheme based on associated Laguerre polynomials L_n^γ (which have a metric $e^{-x}x^\gamma$). Using the theory outlined in the previous section it is clear that $x^{1/2-\gamma}$ and $x^{3/2-\gamma}$ must be whole powers of x and hence that $\gamma-\frac{1}{2}$ must be zero or a negative integer. However, since associated Laguerre polynomials are only defined in terms of $\gamma > -1$, γ can only by $\pm\frac{1}{2}$. We have chosen to use $\gamma=\frac{1}{2}$. The value of M should be chosen to ensure that all the orthonormality integrals implicit in the DVR calculations are still evaluated correctly under the new quadrature scheme. In this case, this means using at least one more point than was used in the orig-

inal DVR calculations. We have tested the stability of the new quadrature scheme by doubling the number of points used. The results were exactly the same, indicating that it is well-behaved.

Once a satisfactory quadrature scheme had been devised, A coefficients were calculated using the DVR wavefunctions and the dipole surfaces of Meyer, Botschwina and Burton (MBB [1]) and of Jensen and Spirko [22]. Table 1 presents the results for transitions between low-lying states, and compares them with calculations of some other workers. Only the calculations by Carney and Porter (CP [15]) did not use Eckart axes (at least explicitly), but it is clear that this approximation does not significantly affect the results. The calculations by Dinelli et al. (DMT [16]) used the same MBB surfaces as were used to produce the results in column 5, but the wavefunctions were produced using the FBR (finite basis representation). The sets of two numbers in columns 5, 6 and 7 result from the symmetry breaking of our calculations – if the upper state is of E symmetry, then two separate A coefficients may be calculated. This demonstrates a problem with the published MBB dipole surface as it stands: it does not have the correct symmetry for H_3^+, resulting in the disagreement between the sets of coefficients quoted in column 5. Once the dipole surface had been corrected [23], by replacing equation (12) in the MBB paper by

$$[d_x, d_y] = \sum_{n,m,k} d_{nmk} S_a^n S_e^{2m+k} \times [\cos k\phi, (-1)^{k-1} \sin k\phi] , \quad (9)$$

the agreement is much better as demonstrated by the results in column 6.

The results presented in section 4 have all been calculated using the MBB dipole surface and DVR wavefunctions calculated from a Hamiltonian of dimension 6500. Comparisons with results obtained from the Jensen dipole surface (see table 1, column 7 and table 2) and with results from DVR wavefunctions calculated from a Hamiltonian of dimension 6000 show that the salient features of figs. 1 and 2 remain. For example the root-mean-square percentage difference, once the very small A coefficients ($<10^{-8}$) have been excluded, between the 6000 and 6500 results is 11%. Absolute agreement between results calculated using the MBB dipole surface and the Jensen dipole surface is less good: A coefficients for the latter are significantly larger than the values used in the figures (see table 2). Nevertheless, the striking structure shown in the figures remains.

4. Results

In fig. 1 the A coefficients for transitions to the ground state are plotted as a function of band origin. The A coefficients are plotted on a log scale in order that the relatively low coefficients for the high-lying states may be seen. It is clear from this figure that the A coefficients drop off much more slowly than is usual for other molecules, which goes part way to explaining why there has been so much success lately in observing up to $\Delta v=3$ transitions (see, for example, ref. [24]). The A coefficients which drop off approximately in a log fashion with frequency are due to transitions from E states, which are symmetry allowed. Transitions from A states, which are symmetry forbidden, contribute to the gradually rising scar of A coefficients. It would appear that around 30000 cm^{-1} the A and E states gradually become indistinguishable from each other in the main. The interesting feature to note from this graph is the regular pattern of transitions with higher than average brightness, spaced about 1800 cm^{-1} apart. Inspection of the bright states shows that each peak is associated with a horseshoe state. Only the horseshoes with 14–20 quanta show clearly in this figure, but it

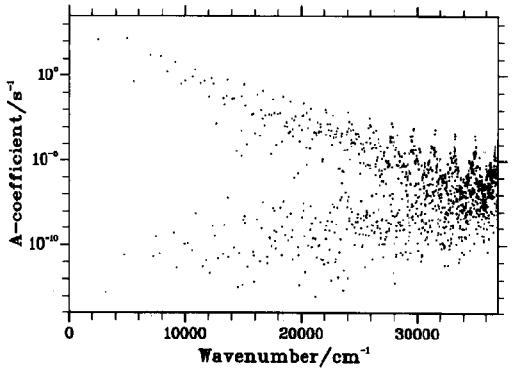

Fig. 1. Einstein A coefficients for transitions to the ground vibrational state, plotted as a function of upper state band origin in wavenumbers. Note the log scale used for the A coefficients.

is possible to pick out a full sequence of horseshoe states (see fig. 3 and table 2), extending all the way from below linearity (where they may be assigned conventionally) to above dissociation, merely by searching for A coefficients that are larger than average.

Fig. 2 shows similar plots to that in fig. 1, but using other low-lying states as the lower state in the transition. It is interesting to see that the variations in brightness which showed so strongly in fig. 1 gradually decrease as more quanta of stretch are put into the lower state (figs. 2a, 2c and 2d), until by the time that there are three quanta of stretch in the lower state, it has all but disappeared. When the lower state is of E symmetry, as in fig. 2b, all transitions are symmetry allowed, and hence the scar due to the symmetry forbidden A↔A transitions apparent in the other plots is missing in this plot.

It would thus appear that the strong transitions are to high bending overtones. These are already known to be strong for the second to fourth overtones [10]. Exciting the stretch turns these transitions into difference transitions and greatly reduces their strength.

Because of vibrational angular momentum, there are several "horseshoe" states with similar model structures even in an unperturbed model. Not all of these have E symmetry. Furthermore, the coupling to the bath also causes the horseshoe scar to be spread over several states. naming a particular state as *the* horseshoe state is therefore largely a subjective matter. The states plotted in fig. 3 are actually the E states with the strongest horseshoe character. As can be seen from fig. 4, the presence of a horseshoe scar correlates well with a high A coefficient.

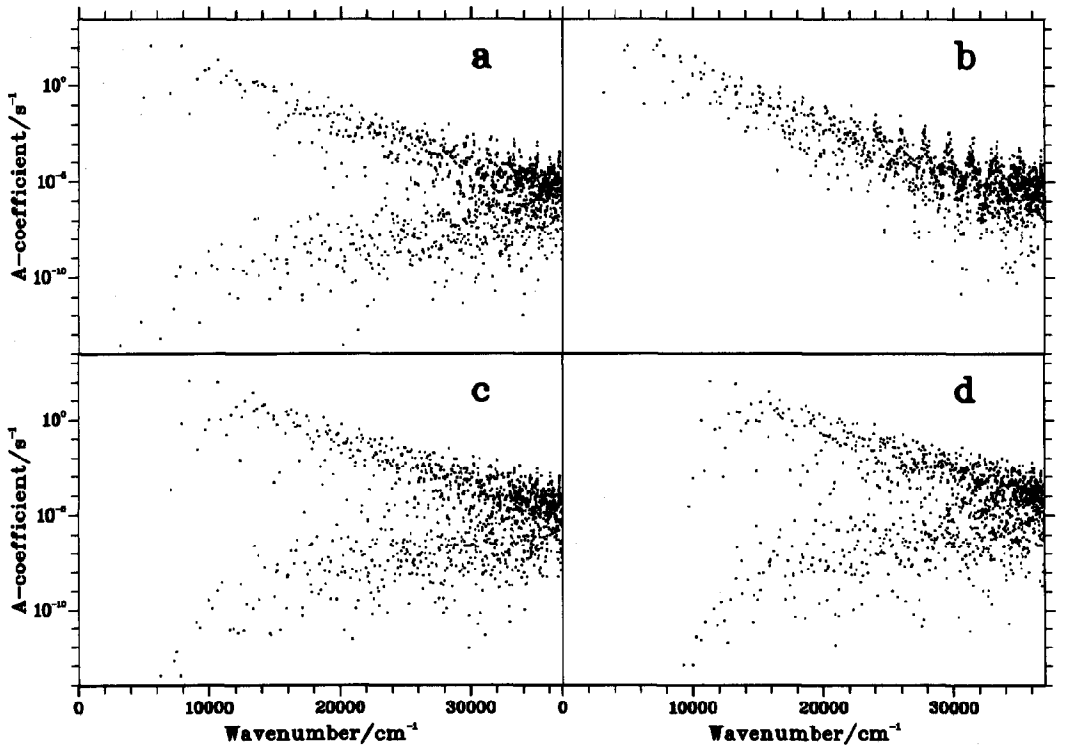

Fig. 2. Einstein A coefficients for transitions to low-lying vibrational states: (a) to the (1, 0^0) state; (b) to the (0, 1^1) state; (c) to the (2, 0^0) state and (d) to the (3, 0^0) state. Note the log scale used for the A coefficients. The horizontal scale is again the band origin of the upper state in wavenumbers, making comparisons between the various graphs slightly easier.

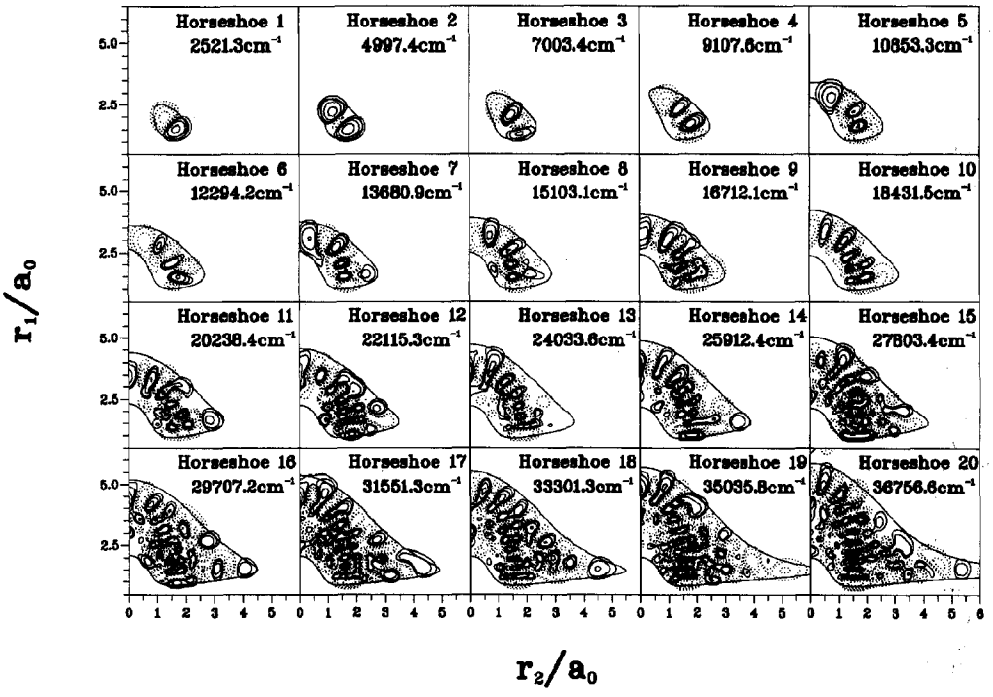

Fig. 3. Contour plots of the upper (even) states of the bright transitions observed in fig. 1 in scattering coordinates, with θ fixed at 90° (plots of odd states in this configuration are meaningless since they are defined to be zero). The band origin of each state is given. Note that the classical turning point allows the possibility of linear configurations ($r_2=0$) from horseshoe 5 onwards. On reflecting through the $r_2=0$ ordinate, the "horseshoe" epithet becomes plain.

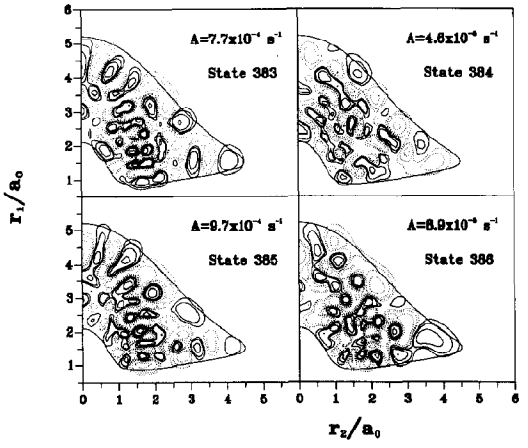

Fig. 4. Even eigenstates in the immediate vicinity of the horseshoe with 16 quanta in the bend, plotted in scattering coordinates with θ fixed at 90° (plots of odd states in this configuration are meaningless since they are defined to be zero). The A coefficient for the transition to the ground state is also given. States 383 and 385 are brighter than states 384 and 386 and have horseshoe character (state 383 is given in fig. 3 and table 2 as *the* horseshoe).

5. Conclusions

Although the potential and dipole surfaces used in this study are not absolutely accurate at energies near dissociation (in particular the MBB potential is known to dissociate to too high a dissociation limit, and the dipole surface behaves incorrectly at geometries where all three atoms are well separated), we feel that the features we have observed are true to the nature of H_3^+. In other words, we believe that there is a highly harmonic series of bright levels resulting from bending motion of the quasi-linear molecule, which provide a gateway in intensity to the surrounding bath of (normally) dark states. We are confident that given enough sensitivity, these transitions could be observed.

Acknowledgement

This work was produced on a IBM RS/6000 work-

station and the Convex C38400 at the University of London Computer Centre. We thank N.G. Fulton for providing the program with which the contour plots in figs. 2 and 4 were produced. We are grateful to the SERC for funding this research through grants GR/G01874 and GR/H41744.

References

[1] W. Meyer, P. Botschwina and P.G. Burton, J. Chem. Phys. 84 (1986) 891.
[2] J.R. Henderson, J. Tennyson and B.T. Sutcliffe, J. Chem. Phys. (1993), in press.
[3] P. Drossart, J.-P. Maillard, J. Caldwell, S.J. Kim, J.K.G. Watson, M.A. Majewski, J. Tennyson, S. Miller, S. Atreya, J. Clarke, J.H. Waite Jr. and R. Wagener, Nature 340 (1989) 539.
[4] A. Carrington and R.A. Kennedy, J. Chem. Phys. 81 (1984) 91.
[5] A. Carrington, I.R. McNab and Y.D. West, J. Chem. Phys. 98 (1993) 1073.
[6] J. Tennyson, O. Brass and E. Pollak, J. Chem. Phys. 92 (1990) 3005.
[7] J.M. Gomez Llorente and E. Pollak, J. Chem. Phys. 90 (1989) 5406.
[8] R.M. Whitnell and J.C. Light, J. Chem. Phys. 90 (1989) 1774.
[9] J. Tennyson and J.R. Henderson, J. Chem. Phys. 91 (1989) 3815.
[10] S. Carter and W. Meyer, J. Chem. Phys. 93 (1990) 8902.
[11] J.R. Henderson and J. Tennyson, Chem. Phys. Letters 173 (1990) 133.
[12] P.N. Day and D.G. Truhlar, J. Chem. Phys. 95 (1991) 6615.
[13] Z. Bačić and J.Z.H. Zhang, Chem. Phys. Letters 184 (1991) 513.
[14] C.R. Le Sueur, S. Miller, J. Tennyson and B.T. Sutcliffe, Mol. Phys. 76 (1992) 1147.
[15] G.D. Carney and R.N. Porter, J. Chem. Phys. 65 (1976) 3547.
[16] B.M. Dinelli, S. Miller and J. Tennyson, J. Mol. Spectry. 153 (1992) 718.
[17] A.S. Dickinson and P.R. Certain, J. Chem. Phys. 49 (1968) 4209.
[18] R.N. Zare, Angular momentum (Wiley–Interscience, New York, 1988).
[19] E.B. Wilson Jr., J.C. Decius and P.C. Cross, Molecular vibrations (Dover, New York, 1980).
[20] J.R. Henderson, C.R. Le Sueur and J. Tennyson, Comput. Phys. Commun. (1993), in press.
[21] M.J. Bramley, J.R. Henderson, J. Tennyson and B.T. Sutcliffe, J. Chem. Phys., submitted for publication.
[22] P. Jensen and V. Špirko, J. Mol. Spectry. 118 (1986) 208.
[23] W. Meyer, private communication.
[24] S.S. Lee, B.F. Ventrudo, D.T. Cassidy, T. Oka, S. Miller and J. Tennyson, J. Mol. Spectry. 145 (1991) 222.